Thioxophosphane (HP=S) and Selenoxophosphane (HP=Se) Complexes of Os(0): Synthesis, Structure, Reactivity, and Theoretical Studies of $Os(\eta^2\text{-}PR{=}E)(CO)_2(PPh_3)_2$ (E = S, R = H, Me; E = Se, R = H)

D. Scott Bohle, Clifton E. F. Rickard, Warren R. Roper,* and Peter Schwerdtfeger

Department of Chemistry, The University of Auckland, Private Bag, Auckland, New Zealand

Received December 28, 1989

The thioxophosphane and selenoxophosphane complexes $Os(\eta^2\text{-}PH{=}E)(CO)_2(PPh_3)_2$ (E = S, **2a**; E = Se, **2b**) are prepared by the sequential addition of triflic acid and base to $Os(O_2CCH_3)(PH_2{=}E)(CO)_2(PPh_3)_2$ (E = S, **1a**; E = Se, **1b**). The $^{31}P\{^1H\}$ NMR spectra of **2a,b** have strongly coupled inequivalent trans triphenylphosphine ligands. Compound **2a** crystallizes in the triclinic space group $P\bar{1}$ with a = 10.524 (4) Å, b = 18.010 (3) Å, c = 10.389 (5) Å, α = 103.26 (3)°, β = 115.63 (3)°, γ = 76.11 (2)°, V = 1705.6 Å^3, and ρ(calcd) = 1.62 g cm^{-3}. The crystal structure of **2a** indicates that both phosphorus and sulfur of HPS lie in the same plane as the osmium and the carbon monoxide ligands. These structural features are interpreted as arising from the binding of HP=S as a π-accepting ligand with a lone pair localized on the phosphorus. Electrophiles such as H^+, Me^+, and AuI add to this lone pair to give the adducts **3**, **7**, and **8**, respectively. In a reversible reaction, acid in the presence of alcohol cleaves the P–S bond in **2a** to give $[Os(PH_2OR)(SH)(CO)_2(PPh_3)_2]^+$ (**4–6**). Deprotonation of the cationic complex containing η^2-PHMe=S, **7a**, returns the neutral complex $Os(\eta^2\text{-}PMe{=}S)(CO)_2(PPh_3)_2$ (**9**), which readily isomerizes to a complex (**10**) with cis triphenylphosphine ligands. A similar fluxionality is also found for the products of the reaction of **10** with acid and methyl triflate. Ab initio SCF calculations for RP=X (R = H, Me; X = CH_2, NH, O, S, Se) at the 6-311+G* level, with and without the second-order Møller–Plesset correction (MP2), are used to determine the structure and the order of frontier orbitals of these species and to rationalize the reactivity of **2a,b** and **10**.

Introduction

It is now well recognized that the use of kinetically stabilizing bulky substituents allows for the isolation of phosphaalkenes ($RP{=}CR_2$), silenes ($R_2Si{=}SiR_2$), and phosphenes (RP=PR) as stable compounds. It is significant then that the analogous low-valent compounds with formal double bonds to oxygen or sulfur, that is oxophosphanes (RP=O), thioxophosphanes (RP=S), and silanones ($R_2Si{=}O$), are known only as reactive intermediates even when bulky substituents are present.[1-3] While an important factor in the stability of these species is the absence of substituents at the sulfur or oxygen, another consideration is the general paucity of low-temperature synthetic routes to such species.

Low-valent organometallic fragments are also able to stabilize otherwise reactive intermediates by providing not only additional kinetic stabilization but also strong π back-bonding. Thus, phosphenes such as HP=PH in $Cp_2Mo(\eta^2\text{-}P_2H_2)$[4] and oxophosphanes such as $R_2NP{=}O$ in $R_2NP(O)Cr(CO)_5$ (R = *i*-Pr)[5] form stable complexes and allow for an assessment of their ligand character and reactivity. The three prior examples of thioxophosphane complexes are all dinuclear species where the ligand is stabilized both by η^2 bonding and by σ coordination to a second metal. Herein we describe (1) the preparation and characterization of a mononuclear osmium complex with the thioxophosphane ligand, HP=S, which is the parent of the class, (2) the unusual reactions of this complex, which include reversible acid cleavage of the P–S bond to give an alkyl phosphinite (PH_2OR) and a thiol (SH) ligand, and (3) ab initio SCF calculations including correlation by a second-order Møller–Plesset perturbation procedure (MP2) for the species RP=X (R = H, Me; X = O, S, Se, NH, CH_2), which clarify the ligand character of these simple species. Some aspects of this work have been communicated.[6]

Scheme I

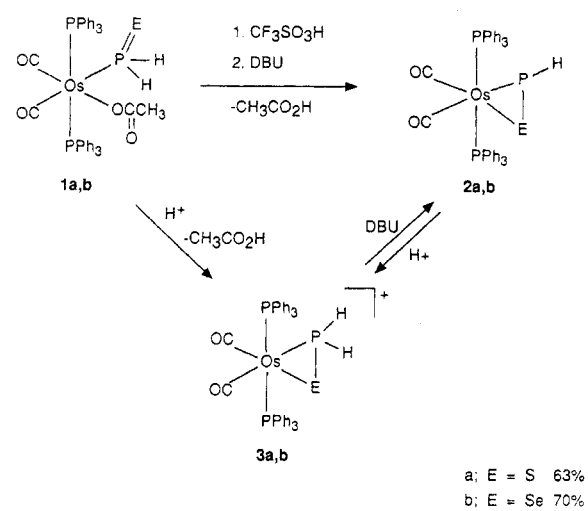

Results and Discussion

The preparation of the thioxo- and selenoxophosphane complexes $Os(\eta^2\text{-}PHE)(CO)_2(PPh_3)_2$ (**2a**, E = S; **2b**, E = Se) is outlined in Scheme I. High yields of **2a,b** are obtained by sequential addition of triflic acid and the nonnucleophilic base DBU (1,8-diazabicyclo[5.4.0]undecene) to suspensions of **1a,b** in dry THF. The complexes **2a,b**

(1) Stille, J. K.; Eichelberger, J. L.; Higgins, J.; Freeburger, M. E. *J. Am. Chem. Soc.* **1972**, *94*, 4761.
(2) Quin, L. D.; Szewczyk, J. *J. Chem. Soc., Chem. Commun.* **1986**, 844.
(3) Hussong, R.; Heydt, H.; Regitz, M. *Phosphorus Sulfur Relat. Elem.* **1985**, *25*, 201.
(4) Cannillo, E.; Coda, A.; Prout, K.; Daran, J. C. *Acta Crystallogr.* **1977**, *B33*, 2608.
(5) Niecke, E.; Englemann, M.; Zorn, H.; Krebs, B.; Henkel, G. *Angew. Chem., Int. Ed. Engl.* **1980**, *19*, 710.
(6) Bohle, D. S.; Rickard, C. E. F.; Roper, W. R. *Angew. Chem., Int. Ed. Engl.* **1988**, *27*, 302; *Angew. Chem.* **1988**, *100*, 308.

0276-7333/90/2309-2068$02.50/0

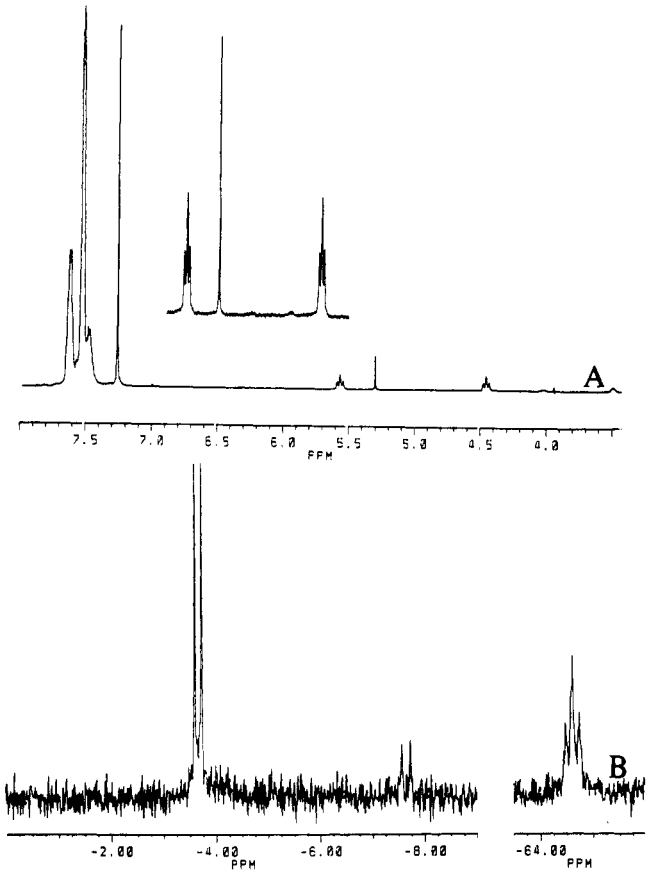

Figure 1. ^1H and $^{31}P\{^1H\}$ NMR spectra for $[Os(\eta^2\text{-}PH_2S)(CO)_2(PPh_3)_2]^+$ (**3**): (A) ^1H spectrum showing PPh_3, H_2PS, $CHCl_3$, and CH_2Cl_2 signals; (B) $^{31}P\{^1H\}$ spectrum for **3** generated in situ (the weak doublet at −7.6 ppm is due to a decomposition product).

are isolated as moderately air-stable pale yellow crystalline solids after recrystallization. Direct reaction of **1a** with base returns only traces (<5%) of **2a**, and attempted dehydrochlorination of the closely related chloride-containing derivative $OsCl(PH_2S)(CO)_2(PPh_3)_2$ returns products that do not include **2a**. These latter observations illustrate the importance of acid labilization of the acetate ligand, which is probably lost as acetic acid, although this was not experimentally verified. A related reaction between perchloric acid and $Os(\eta^1\text{-}OC(O)Me)(PH_2)(CO)_2(PPh_3)_2$ also results in acetate elimination, although in this case the ligand cannot fill the vacant coordination site and other reactions occur.[7] Also shown in Scheme I is the intermediate **3a**, which has been spectroscopically characterized (see Tables VI and VII). Thus, addition of triflic acid to either **1a** or **2a** can be shown by ^1H and ^{31}P NMR spectroscopy (Figure 1) to lead to the same species, which has equivalent triphenylphosphine ligands. Notable features of these spectra are (1) the low-field shift of the protons of the $\eta^2\text{-}PH_2S$ ligands (δ = 5.01 ppm), (2) the strong $^1J_{HP}$ = 444.7 Hz, and (3) the chemical shift of the phosphorus of the $\eta^2\text{-}PH_2S$ ligand (δ = −64.6 ppm). Samples of **3a** decompose within 30 min of preparation to give undetermined products. Regardless of the method of preparation of **3a**, addition of excess DBU to its solutions results in instantaneous formation of the signals of **2a** in the ^1H and ^{31}P NMR spectra. The related intermediate **3b** is probably present in the preparation of **2b**.

Spectroscopic Characterization of 2a,b. In formal terms the complexes **2a,b** can be classified either as Os(II)

(7) Bohle, D. S.; Clark, G. R.; Rickard, C. E. F.; Roper, W. R. Submitted for publication in *J. Organomet. Chem.*

Table I. Carbonyl Stretching Bands for π Adducts of $Os(CO)_2(PPh_3)_2$

complex	ν(CO), cm^{-1}	Δ, cm^{-1}	ref
$Os(CS_2)(CO)_2(PPh_3)_2$	2000, 1940	60	31
$Os(C(=NPh)S)(CO)_2(PPh_3)_2$	2000, 1935	65	32
$Os(S_2)(CO)_2(PPh_3)_2$	1998, 1944	54	33
$Os(Se_2)(CO)_2(PPh_3)_2$	2000, 1937	63	34
$Os(PHS)(CO)_2(PPh_3)_2$	1989, 1922	67	this work
$Os(PHSe)(CO)_2(PPh_3)_2$	1987, 1924	63	this work
$Os(PhC_2Ph)(CO)_2(PPh_3)_2$	1980, 1900	80	31
$Os(CH_2O)(CO)_2(PPh_3)_2$	1977, 1902	75	13
$Os(C_2H_4)(CO)_2(PPh_3)_2$	1955, 1895	60	35

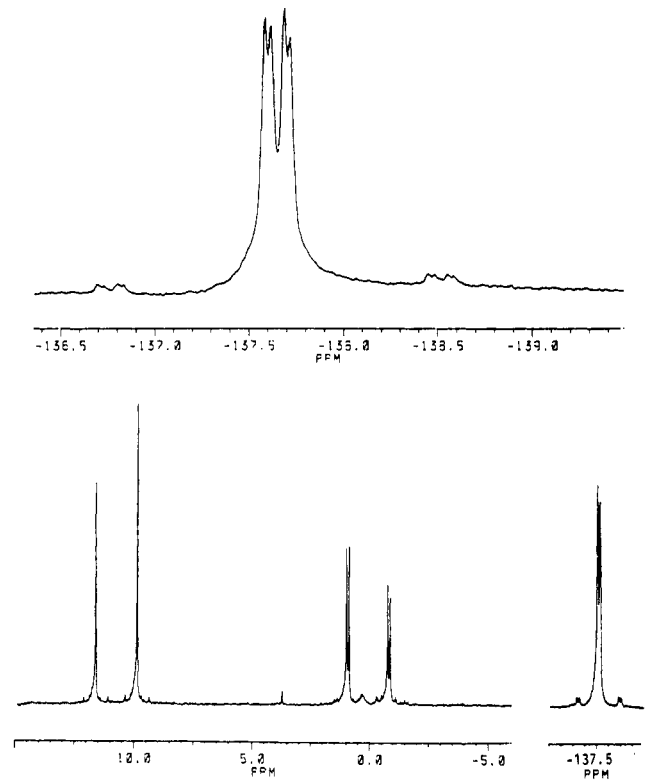

Figure 2. Complete $^{31}P\{^1H\}$ NMR spectrum for $Os(\eta^2\text{-}PHSe)(CO)_2(PPh_3)_2$ (**2b**) showing an AB quartet pattern for triphenylphosphine ligands (below) and an expanded section of the selenoxophosphane resonance showing flanking ^{77}Se satellites (above).

complexes of the dianion HPS^{2-} or as Os(0) π complexes of a neutral HP=S ligand. In Table I the carbonyl stretching modes for these complexes are contrasted with those of related π adducts of the $Os(CO)_2(PPh_3)_2$ fragment. These data suggest that the electronic environment in **2a,b** is similar to that in the Os(0) adducts of diphenylacetylene and disulfur. Observed vibrational modes for the HP=E ligands are limited to ν(P–H), which have remarkably low values of 2196 and 2202 cm^{-1} for **2a** and **2b**, respectively. Unfortunately the δ(P–H) deformation mode and the P–S stretching frequency are obscured by the broad triphenylphosphine bands between 800 and 500 cm^{-1}. In valence bond terms the low frequencies for ν(P–H) in these ligands can be attributed to decreased phosphorus 3s participation in the P–H bond. This theme will be developed further in the discussion of the ab initio calculations for these species.

Weak P–H bonding is also implied by the ^1H NMR spectroscopic results for **2a,b**. In these complexes the direct one-bond hydrogen–phosphorus couplings, $^1J_{HP}$ = 117.5 and 118.5 Hz for **2a,b**, respectively, are among the lowest reported. The chemical shift of these protons, $\delta(^1H)$ = 0.82 ppm for **2a**, is at a considerably higher field than for **3a** (shown in Figure 1). The two $^3J_{H\text{-}PPh_3}$ coupling

Table II. $^{77}Se\{^1H\}$ **NMR Data**[a]

	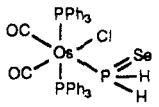	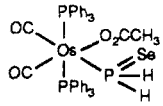	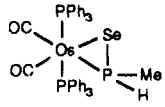	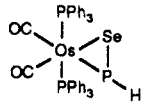
δ, ppm	−364	−413	−672	−472
$^1J_{PSe}$, Hz	517	531	422	280
$^2J_{PSe}$, Hz			14.3, 6.2	9.5, 4.4

[a] δ with respect to Me_2Se.

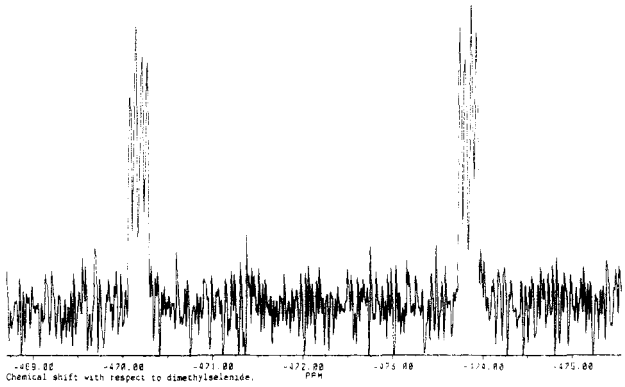

Figure 3. $^{77}Se\{^1H\}$ NMR spectrum for $Os(\eta^2\text{-}PHSe)(CO)_2(PPh_3)_2$ (**2b**).

constants do not differ significantly, and the resulting peak retains an overall doublet of triplets pattern.

The ^{31}P NMR spectrum, shown in Figure 2 for **2b**, is dominated by the inequivalence of the triphenylphosphine ligands and by the upfield shift of the HPE resonance. This inequivalence is accompanied by a strong mutual coupling, $^2J_{PPh_3\text{-}PPh_3}$ = 282.4 Hz for **2b**, and a different coupling to the HPE phosphorus. In Figure 2 the ^{31}P resonance for the selenoxophosphane ligand is expanded and the ^{77}Se satellites are clearly visible. The direct one-bond P–Se coupling reflected by these values is confirmed by the measurement of the ^{77}Se NMR spectrum, which is shown in Figure 3. Related ^{77}Se NMR results are collected and contrasted in Table II, and the most significant feature of these data is the relative magnitude of the diminished P–Se coupling for **2b**. This coupling is also well below the range found for selenoxophosphoranes $R_3P{=}Se$, $^1J_{PSe}$ = 684–1053 Hz, and is comparable to the range found for P–Se single bonds such as in $R_2P\text{–}SeR$, where $^1J_{PSe}$ = 205–341 Hz.[8]

Structural Characterization of $Os(\eta^2\text{-}PHS)(CO)_2(PPh_3)_2$. In order to ascertain the exact orientation of the thioxophosphane ligand in **2a**, the structure was determined by single-crystal X-ray diffraction. The full molecular (Schakal) representation of **2a** (Figure 4) clearly indicates that the phosphorus and sulfur are coplanar with the carbon monoxide ligands. Unfortunately the phosphorus-bound proton was not located by Fourier difference techniques and the refined parameters do not allow for a distinction to be made between the phosphorus and the sulfur, here labeled PS(1) and PS(2). In spite of this problem the refinement converged to the final residuals of R = 0.0398 and R_w = 0.0409, and the crystallographic parameters for the two atoms do not reflect disorder. Bond lengths and angles and atomic positional parameters are collected in Tables III–V, respectively. Crystallographic data collection parameters are described in the Experimental Section.

(8) McFarlane, H. C. E.; McFarlane, W. *NMR of Newly Accessible Nuclei*; Academic: New York, 1982; Vol. 2, p 275.

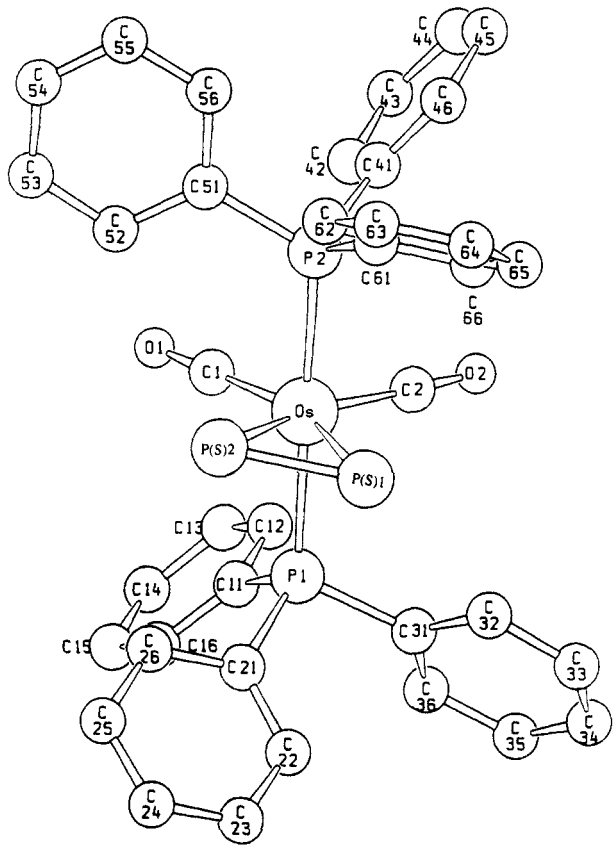

Figure 4. Molecular structure of $Os(\eta^2\text{-}PHS)(CO)_2(PPh_3)_2$ (**2a**).

Table III. Interatomic Distances (Å) for $Os(\eta^2\text{-}PHS)(CO)_2(PPh_3)_2$

Bond Lengths Involving Osmium					
Os–P(1)	2.403 (3)	Os–PS(1)	2.457 (3)	Os–C(1)	1.897 (12)
Os–P(2)	2.394 (3)	Os–PS(2)	2.443 (3)	Os–C(2)	1.908 (12)

Bond Lengths Involving the Thioxophosphane and Carbonyl Ligands					
PS(1)–PS(2)	2.090 (5)	C(1)–O(1)	1.149 (13)	C(2)–O(2)	1.138 (13)

Bond Lengths Involving the Triphenylphosphine Ligands			
P(1)–C(11)	1.837 (11)	P(2)–C(41)	1.837 (11)
P(1)C(21)	1.809 (11)	P(2)–C(51)	1.810 (10)
P(1)–C(31)	1.839 (10)	P(2)–C(61)	1.818 (11)

	i					
	1	2	3	4	5	6
C(*i*1)–C(*i*2)	1.39 (2)	1.38 (2)	1.38 (2)	1.40 (2)	1.40 (2)	1.41 (2)
C(*i*1)–C(*i*6)	1.39 (2)	1.41 (2)	1.39 (2)	1.37 (2)	1.41 (2)	1.39 (2)
C(*i*2)–C(*i*3)	1.41 (2)	1.42 (2)	1.42 (2)	1.42 (2)	1.43 (2)	1.43 (2)
C(*i*3)–C(*i*4)	1.38 (2)	1.36 (2)	1.36 (2)	1.37 (2)	1.38 (2)	1.36 (2)
C(*i*4)–C(*i*5)	1.37 (2)	1.38 (2)	1.38 (2)	1.38 (2)	1.36 (2)	1.34 (2)
C(*i*5)–C(*i*6)	1.44 (2)	1.46 (2)	1.43 (2)	1.43 (2)	1.40 (2)	1.43 (2)

The thioxophosphane ligand is bound with almost identical metal–sulfur and metal–phosphorus bond lengths (Os–PS(1) = 2.457 (3) Å; Os–PS(2) = 2.443 (3) Å) and contains a long phosphorus–sulfur bond length (PS(1)–PS(2) = 2.090 (5) Å). This bond length is considerably longer than that found for thiophosphoryl compounds, 1.86–1.94 Å,[9] and is within the range usually associated

Table IV. Bond Angles for $Os(\eta^2\text{-PHS})(CO)_2(PPh_3)_2$ (deg)

Angles at the Osmium			
P(1)–Os–P(2)	176.9 (1)	C(1)–Os–PS(1)	156.3 (3)
P(1)–Os–PS(1)	86.4 (1)	C(1)–Os–PS(2)	106.2 (3)
P(2)–Os–PS(1)	90.6 (1)	C(2)–Os–P(1)	89.5 (3)
P(1)–Os–PS(2)	93.3 (1)	C(2)–Os–P(2)	91.6 (3)
P(2)–Os–PS(2)	84.6 (1)	C(2)–Os–PS(1)	107.3 (3)
PS(1)–Os–PS(2)	50.5 (1)	C(2)–Os–PS(2)	157.2 (3)
C(1)–Os–P(1)	91.5 (3)	C(1)–Os–C(2)	96.3 (5)
C(1)–Os–P(2)	91.2 (3)		
Angles within the Thioxophosphane and Carbonyl Ligands			
PS(1)–PS(2)–Os	65.1 (1)	Os–C(1)–O(1)	178.9 (1.0)
PS(2)–PS(1)–Os	64.4 (1)	Os–C(2)–O(2)	177.7 (1.0)
Angles at Phosphorus in Triphenylphosphine Ligands			
Os–P(1)–C(11)	111.4 (3)	Os–P(2)–C(41)	114.3 (3)
Os–P(1)–C(21)	119.4 (3)	Os–P(2)–C(51)	117.7 (4)
Os–P(1)–C(31)	114.4 (4)	Os–P(2)–C(61)	114.6 (4)
C(11)–P(1)—C(21)	105.2 (5)	C(41)–P(2)–C(51)	100.2 (5)
C(11)–P(1)–C(31)	102.6 (5)	C(41)–P(2)–C(61)	104.4 (5)
C(21)–P(1)–C(31)	102.0 (5)	C(51)–P(2)–C(61)	103.8 (5)

Table V. Atomic Positional Parameters for $Os(\eta^2\text{-PHS})(CO)_2(PPh_3)_2$

atom	*x/a*	*y/b*	*z/c*
Os	0.25799 (5)	0.24910 (3)	0.03099 (5)
P(1)	0.3613 (3)	0.3547 (2)	0.2045 (3)
P(2)	0.1595 (3)	0.1455 (2)	−0.1505 (3)
PS(1)	0.3638 (4)	0.2779 (2)	−0.1178 (3)
PS(2)	0.1489 (4)	0.3251 (2)	−0.1693 (4)
C(1)	0.1181 (13)	0.2591 (7)	0.1056 (12)
O(1)	0.0317 (11)	0.2650 (6)	0.1485 (10)
C(2)	0.3977 (12)	0.1783 (7)	0.1539 (12)
O(2)	0.4781 (10)	0.1342 (6)	0.2248 (10)
C(11)	0.2988 (11)	0.3784 (6)	0.3513 (11)
C(12)	0.3148 (13)	0.3187 (7)	0.4244 (13)
C(13)	0.2643 (15)	0.3334 (8)	0.5352 (15)
C(14)	0.2044 (17)	0.4075 (9)	0.5731 (17)
C(15)	0.1863 (17)	0.4673 (10)	0.5019 (18)
C(16)	0.2344 (15)	0.4527 (9)	0.3873 (16)
C(21)	0.3374 (15)	0.4460 (6)	0.1457 (11)
C(22)	0.4512 (13)	0.4821 (8)	0.1753 (13)
C(23)	0.4251 (15)	0.5534 (9)	0.1248 (15)
C(24)	0.2908 (17)	0.5871 (9)	0.0449 (17)
C(25)	0.1740 (17)	0.5532 (9)	0.0131 (17)
C(26)	0.1971 (15)	0.4798 (9)	0.0632 (16)
C(31)	0.5564 (15)	0.3341 (6)	0.3016 (11)
C(32)	0.6399 (14)	0.2943 (8)	0.2278 (14)
C(33)	0.7905 (15)	0.2857 (8)	0.2997 (16)
C(34)	0.8532 (15)	0.3096 (8)	0.4432 (15)
C(35)	0.7718 (15)	0.3470 (8)	0.5208 (15)
C(36)	0.6197 (13)	0.3597 (7)	0.4484 (14)
C(41)	0.1965 (11)	0.0536 (6)	−0.0826 (12)
C(42)	0.1688 (14)	0.0558 (8)	0.0388 (14)
C(43)	0.1859 (15)	−0.0130 (9)	0.0921 (16)
C(44)	0.2322 (17)	−0.0814 (9)	0.0238 (17)
C(45)	0.2567 (17)	−0.0861 (9)	−0.0984 (18)
C(46)	0.2386 (16)	−0.0161 (9)	−0.1516 (16)
C(51)	−0.0328 (11)	0.1562 (6)	−0.2440 (11)
C(52)	−0.1225 (12)	0.2233 (7)	−0.2174 (13)
C(53)	−0.2738 (13)	0.2287 (7)	−0.2958 (13)
C(54)	−0.3277 (15)	0.1675 (8)	−0.3982 (15)
C(55)	−0.2422 (15)	0.1016 (8)	−0.4248 (15)
C(56)	−0.0939 (12)	0.0942 (7)	−0.3462 (13)
C(61)	0.2220 (11)	0.1211 (6)	−0.2953 (12)
C(62)	0.1297 (13)	0.1385 (7)	−0.4347 (13)
C(63)	0.1894 (14)	0.1242 (8)	−0.5403 (14)
C(64)	0.3297 (15)	0.0939 (8)	−0.5067 (15)
C(65)	0.4177 (15)	0.0770 (8)	−0.3739 (16)
C(66)	0.3657 (13)	0.0910 (7)	−0.2629 (13)

with P–S single bonds. The metal fragment retains an almost perfect octahedral geometry with respect to the carbonyl and triphenylphosphine ligands. The PS(1)–P-S(2) orientation is symmetric with respect to this octahedron so that PS(2)–Os–C(1) = 106.2 (3)° and PS(1)–Os–C(2) = 107.3 (3)°.

As seen in the closely related formaldehyde complex $Os(\eta^2\text{-}CH_2O)(CO)_2(PPh_3)_2$, phosphorus and sulfur are coplanar with the metal and the carbonyl ligands. Furthermore, the largest out-of-plane distortion from the plane defined by Os, C(1), C(2), PS(1), and PS(2) is 0.08 Å by PS(2) and the values for the other atoms are all of comparable magnitude. These results clearly indicate that the observed inequivalence of the triphenylphosphine ligands is due to the inherent asymmetry of the HPS ligand with respect to the plane defined by the metal and thioxophosphane ligand. We attribute this to the presence of a spatially directed lone pair on one side and the phosphorus-bound proton on the other side of the aforementioned plane. The observation of triphenylphosphine inequivalence at 25 °C also suggests that inversion of the phosphorus geometry must be slow on the NMR time scale.

The other thioxophosphane complexes that have been reported are dinuclear species which contain the skeleton depicted in A. The structural data for these three com-

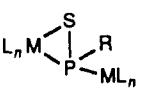

A

plexes are contrasted with those found for **2a** in Table VIII. There are two significant features of this comparison: (1) there is a considerably longer phosphorus–sulfur bond length in **2a** as compared to those in the dinuclear examples A; (2) in the dinuclear cases there is a significant difference in the metal–phosphorus and metal–sulfur bond lengths. Both of these features are expected for the coordination of the strongly π-accepting HPS ligand to an extremely basic metal fragment.

Thioxophosphanes are, however, potentially ambivalent ligands in that they can bind in two ways (B and C). In

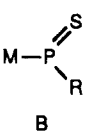

B

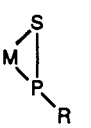

C

the case of B, RP=S can be a η^1-P-bound ligand with essentially good σ-donor but weak π-acceptor characteristics. However, when RP=S is η^2-P- and S-bound as in C, the predominant ligand character is as a good π-acceptor with some π-donor capability. The spectroscopic studies described below, for R = Me, can be rationalized by B ⇌ C interconversion, as a means for facile isomerization of the ligand sphere. A ligand that is closely related to thioxophosphanes, a methylenephosphane, has been described recently in the complex $(C_5Me_5)Rh(\eta^2\text{-}PhP{=}CH_2)(CO)$.[10]

Reactivity Patterns of the Thioxophosphane Complexes. As depicted in Scheme I, **2a,b** are formulated with stereochemically active lone pairs localized on the phosphorus. The best evidence for this formulation is derived from the reactions of these complexes with electrophiles.

As described before, the phosphorus in **2a** is reversibly protonated to give the cationic complex $[Os(\eta^2\text{-}PH_2S)(CO)_2(PPh_3)_2]^+$ (**3a**). On standing, or in the presence of water, this product decomposes, and attempts to recover **2a** by treating these solutions with excess base are un-

(9) Corbridge, D. E. C. *Phosphorus: an Outline of Its Chemistry, Biochemistry and Technology*; Elsevier: Amsterdam, 1985.

(10) Werner, H.; Paul, W.; Wolf, J.; Steinmetz, M.; Zolk, R.; Müller, G.; Steigelmann, O.; Riede, J. *Chem. Ber.* **1989**, *122*, 1061.

Table VI. NMR Spectroscopic Data[a] for New Compounds

compd	^{1}H NMR data	^{31}P NMR data
$Os(\eta^2\text{-}PHS)(CO)_2(PPh_3)_2$ (**2a**)	0.82 (dt, $^1J_{HP}$ = 117.5, $^3J_{HP}$ = 6.6, 1, P*H*S)	−140.4 (dd, $^2J_{PP}$ = 13.9, 6.5, *P*HS) 1.6 (dd, $^2J_{PP}$ = 285.9, 13.9, *P*Ph$_3$) 12.5 (d, $^2J_{PP}$ = 285.9, *P*Ph$_3$)
$Os(\eta^2\text{-}PHSe)(CO)_2(PPh_3)_2$ (**2b**)	0.83 (dt, $^1J_{HP}$ = 118.5 $^3J_{HP}$ = 7.8, 1, P*H*Se)	−137.6 (dd, $^2J_{PP}$ = 16.6, 5.1, *P*HSe) 0.1 (dd, $^2J_{PP}$ = 282.4, $^2J_{PP}$ = 16.6, *P*Ph$_3$) 10.7 (d, $^2J_{PP}$ = 282.4, *P*Ph$_3$)
$[Os(\eta^2\text{-}PH_2S)(CO)_2(PPh_3)_2]CF_3SO_3$ ((**3**)CF_3SO_3)	5.01 (dt, $^1J_{HP}$ = 444.7, $^3J_{HP}$ = 8.7, 2, PH_2S)	−64.6 (t, $^2J_{PP}$ = 21.1, *P*H$_2$S) −3.7 (d, $^2J_{PP}$ = 21.1, *P*Ph$_3$)
$[Os(SH)(PH_2OMe)(CO)_2(PPh_3)_2]ClO_4$ ((**4**)ClO_4)	−2.91 (td, $^2J_{HP}$ = 11.2, $^2J_{HP}$ = 3.2, 2, Os*H*) 3.29 (d, $^3J_{HP}$ = 12.7, 3, POCH_3) 4.41 (dt, $^1J_{HP}$ = 445.5, $^3J_{HP}$ = 8.3, 2, PH_2)	−7.2 (d, $^2J_{PP}$ = 25.0, *P*Ph$_3$) 34.7 (t, $^2J_{PP}$ = 26.5, *P*H$_2$OMe)
$[Os(SH)(PH_2OEt)(CO)_2(PPh_3)_2]ClO_4$ ((**5**)ClO_4)	−2.90 (td, $^3J_{HP}$ = 11.1, 3.6, 1, Os*H*) 1.19 (t, $^3J_{HH}$ = 7.0, 3, CH_3) 3.42 (dq, $^3J_{HH}$ = 7.0, $^3J_{HP}$ = 8.4, 2, CH_2) 4.62 (dt, $^1J_{HP}$ = 442.3, $^3J_{HP}$ = 8.3, 2, PH_2)	−7.4 (d, $^2J_{PP}$ = 26.4, *P*Ph$_3$) 28.0 (t, $^2J_{PP}$ = 26.6, *P*H$_2$OEt)
$[Os(SeH)(PH_2OEt)(CO)_2(PPh_3)_2]ClO_4$ ((**6**)ClO_4)	−5.13 (td, $^3J_{HP}$ = 11.7, $^3J_{HP}$ = 3.0, 1, OsSe*H*) 1.22 (t, $^3J_{HH}$ = 7.0, 3, CH_3) 3.38 (dq, $^3J_{HH}$ = 7.0, $^3J_{HP}$ = 8.2, 2, CH_2) 4.70 (dt, $^1H_{HP}$ = 444.6, $^3J_{HP}$ = 8.6, 2, PH_2)	−7.3 (d, $^2J_{PP}$ = 26.0, *P*Ph$_3$) 21.4 (t, $^2J_{PP}$ = 26.0, *P*H$_2$OEt)
$[Os(\eta^2\text{-}PHMeS)(CO)_2(PPh_3)_2]CF_3SO_3$ ((**7a**)CF_3SO_3)	1.47 (dd, $^2J_{HP}$ = 13.1, $^3J_{HH}$ = 4.7, 3, PCH_3) 3.58 (dm, $^1J_{HP}$ = 475.7, $^3J_{HP}$ = 2.7, 1, P*H*)	−38.7 (t, $^2J_{PP}$ = 22.4, *P*HMeS) −3.9 (dd, $^2J_{PP}$ = 229.2, $^2J_{PP}$ = 21, *P*Ph$_3$) 1.2 (dd, $^2J_{PP}$ = 229.2, $^2J_{PP}$ = 23.6, *P*Ph$_3$)
$[Os(\eta^2\text{-}PHMeSe)(CO)_2(PPh_3)_2]CF_3SO_3$ ((**7b**)CF_3SO_3)	1.56 (dd, $^2J_{HP}$ = 13.0, $^3J_{HH}$ = 4.9, 3, PCH_3) 3.56 (dm, $^1J_{HP}$ = 474.7, 1, P*H*)	−39.1 (t, $^2J_{PP}$ = 21.8, *P*HMeSe) −6.4 (dd, $^2J_{PP}$ = 227.2, $^2J_{PP}$ = 20.2, *P*Ph$_3$) −0.8 (dd, $^2J_{PP}$ = 227.1, $^2J_{PP}$ = 23.3, *P*Ph$_3$)
$Os(PH(AuI)S)(CO)_2(PPh_3)_2$ (**8**)	3.20 (dt, $^1J_{HP}$ = 343.9, $^3J_{HP}$ = 4.8, 1, P*H*(AuI)S)	−72.6 (t, $^2J_{PP}$ = 14.6, *P*H(AuI)S) 4.3 (t, $^2J_{PP}$ = 14.1, *P*Ph$_3$)
At 223 K		−70.8 (m, *P*H(AuI)S) 5.3 (d, $^2J_{PP}$ = 13, *P*Ph$_3$)
trans-$Os(\eta^2\text{-}PMeS)(CO)_2(PPh_3)_2$ (**9**) at 270 K		−46.9 (d, $^2J_{PP}$ = 29.0, *P*MeS) 2.6 (dd, $^2J_{PP}$ = 284.9, $^2J_{PP}$ = 26.6, *P*Ph$_3$) 11.8 (d, $^2J_{PP}$ = 282.9, *P*Ph$_3$)
cis-$Os(\eta^2\text{-}PMeS)(CO)_2(PPh_3)_2$ (**10**) at 295 K		−23.9 (dd, $^2J_{PP}$ = 26.3, 31.1, *P*MeS) −1.0 (tm, $^2J_{PP}$ = 23.6, *P*Ph$_3$) 1.7 (dd, $^2J_{PP}$ = 31.1, $^2J_{PP}$ = 20.32, *P*Ph$_3$)
cis-$[Os(\eta^2\text{-}PHMeS)(CO)_2(PPh_3)_2]$-$CF_3SO_3$ ((**11**)CF_3SO_3)	2.56 (dm, $^2J_{HP}$ = 13.3, 3, PCH_3) 4.00 (dm, $^1J_{HP}$ = 473.3, 1, P*H*)	−24.7 (dd, $^2J_{PP}$ = 143.3, $^2J_{PP}$ = 19.1, *P*HMeS) −6.8 (dd, $^2J_{PP}$ = 143.1, $^2J_{PP}$ = 21.5, *P*Ph$_3$) −1.9 (dm, $^2J_{PP}$ = 22.8, *P*Ph$_3$)
$[Os(\eta^2\text{-}PMe_2S)(CO)_2(PPh_3)_2]CF_3SO_3$ ((**12**)CF_3SO_3)	1.60 (d, $^2J_{HP}$ = 11.7, 6, PCH_3)	−24.9 (t, $^2J_{PP}$ = 23.6, *P*Me$_2$S) 1.1 (d, $^2J_{PP}$ = 23.8, *P*Ph$_3$)

[a] As chloroform solutions at 21 °C. Proton chemical shifts (δ) are given in ppm with respect to tetramethylsilane, and for phosphorus shifts are given in ppm with respect to external 85% H_3PO_4. J values are given in Hz. For ^{77}Se NMR data see Table II.

successful. On the other hand, when **2a** is treated with perchloric acid in alcohol, colorless crystalline products are obtained in very good yields. The products of these reactions (eq 1) are isolated as perchlorate salts and contain

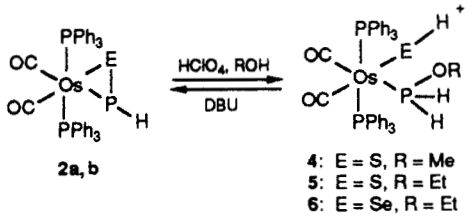

2a, b

4: E = S, R = Me
5: E = S, R = Et
6: E = Se, R = Et

(1)

alkyl phosphinite and thiol ligands, which result from cleavage of the phosphorus–sulfur bond with the net addition of ROH and H^+ to the complex. The identities of **4–6** are unambiguous from NMR and IR spectroscopy and are consistent with the elemental analyses. For example, the IR spectrum of **4** has strong bands at 1030 and 910 cm^{-1} in the ν(P–O) region and has a distinct doublet in the ^{1}H NMR spectrum at δ = 3.2 (d, 3, $^3J_{HP}$ = 12.7 Hz, OCH_3), which indicates a methyl phosphinite ligand. The thiol proton has a unique chemical shift in the ^{1}H NMR spectrum at δ = −2.91 (td, 1, $^3J_{HP}$ = 11.2 and 3.2 Hz, S*H*), and the coupling pattern for this signal arises from two equivalent phosphorus nuclei and a third inequivalent phosphorus. The overall chemical shift range for thiol complexes is δ = −1.1 to −3.8.[11,12]

A remarkable aspect of this reaction is that it is reversible, as addition of an excess of the base DBU to **4** and **5** leads to re-formation of **2a** in very good yield. There are very few examples of reversible bond cleavage and formation for π adducts of transition metals; often either the forward or reverse reaction leads to elimination of one of the fragments. For example, when the formaldehyde complex $Os(\eta^2\text{-}CH_2O)(CO)_2(PPh_3)_2$ is treated with hydroiodic acid, water is lost and the ultimate product is $OsI(CH_2I)(CO)_2(PPh_3)_2$.[13] Alkyl phosphinite complexes are also produced when $M(\eta^1\text{-}OC(O)CH_3)(PH_2)(CO)_2(PPh_3)_2$ (M = Ru, Os) is treated under the same conditions, and we have proposed that a possible intermediate in this reaction (D, Scheme II) contains a planar phosphido species.

(11) Fischer, R. A.; Kneuper, H.-J.; Herrmann, W. A. *J. Organomet. Chem.* **1987**, *330*, 365.
(12) Kury, R.; Vahrenkamp, H. *J. Chem. Res., Synop.* **1982**, 30; *J. Chem. Res., Miniprint* **1982**, 401.
(13) Clark, G. R.; Headford, C. E. L.; Marsden, K.; Roper, W. R. *J. Organomet. Chem.* **1982**, *231*, 335.

Table VII. Infrared Spectroscopic Data[a] for New Compounds

complex	ν(CO)	ν(PH)	other bands
$Os(\eta^2\text{-}PHS)(CO)_2(PPh_3)_2$ (**2a**)	1989, 1922	2196 m	
$Os(\eta^2\text{-}PHSe)(CO)_2(PPh_3)_2$ (**2b**)	1987, 1924	2202 m	
$[Os(SH)(PH_2OMe)(CO)_2(PPh_3)_2]ClO_4$ ((**4**)ClO_4)	2057, 2000	2362 br	1030 m, 970 s (P–OMe)
$[Os(SH)(PH_2OEt)(CO)_2(PPh_3)_2]ClO_4$ ((**5**)ClO_4)	2056, 1998	2357 br	1032 m, 979 m, 944 s (ν(P–OEt))
$[Os(SeH)PH_2OEt)(CO)_2(PPh_3)_2]ClO_4$ ((**6**)ClO_4)	2056, 1998		1031 m, 973 m, 940 s (ν(P–OEt))
$[Os(\eta^2\text{-}PHMeS)(CO)_2(PPh_3)_2]CF_3SO_3$ ((**7a**)CF_3SO_3)	2050, 1978 1957 (s) 1924 (s)		1277 s, 1262 s, 1160 m, 1032 s ($\nu(CF_3SO_3)$) 888 w, 862 w, 805 w (PHMe)
$[Os(\eta^2\text{-}PHMeSe)(CO)_2(PPh_3)_2]CF_3SO_3$ ((**7b**)CF_3SO_3)	2051, 1983 (s) 1957		1278 sh, 1263 s, 1161 m, 1033 s ($\nu(CF_3SO_3)$) 884 w, 863 w, 802 w (PHMe)
$Os(P(AuI)HS)(CO)_2(PPh_3)_2$ (**8**)	2022, 1987 (s) 1940	2271 w	860 m, 849 w (δ(P–H))
trans-$Os(\eta^2\text{-}PMeS)(CO)_2(PPh_3)_2$ (**9**)	1995, 1912		846 w, 807 w (ρ(P–Me))
cis-$Os(\eta^2\text{-}PMeS)(CO)_2(PPh_3)_2$ (**10**)	2021, 1902		1084 sh 863 w, 822 w (ρ(P–Me))
cis-$[Os(\eta^2\text{-}PHMeS)(CO)_2(PPh_3)_2]CF_3SO_3$ ((**11**)CF_3SO_3)	2059, 1973		1000 m, 886 w, 805 w (PHMe)
$[Os(\eta^2\text{-}PMe_2S)(CO)_2(PPh_3)_2]CF_3SO_3$ ((**12**)CF_3SO_3)	2045, 1972		1280 s, 1262 s, 1153 m, 1032 s (CF_3SO_3) 959 m, 901 m, 851 w (ρ(P–Me))

[a] In cm^{-1}; spectra recorded as Nujol mulls between KBr or CsI plates and calibrated with polystyrene. All carbonyl bands are strong unless indicated otherwise; s = strong, m = medium, w = weak, sh = shoulder, (s) = solution spectrum recorded in dichloromethane. Bands due to triphenylphosphine ligands are not included.

Table VIII. Structurally Characterized Thioxophosphane Complexes

complex	bond lengths, Å				bond angles, deg		
	P–S	M–P[a]		M–S	M–P–M	P–M–S	ref
$Cp_2Mo_2(\eta^2\text{-}\mu\text{-}PhPS)(CO)_5$	2.025 (4)	Mo Mo*	2.447 (3) 2.553 (3)	2.544 (3)	132.2 (1)	47.8 (1)	36
$Cp_2Mo_2(\eta^2\text{-}\mu\text{-}RPS)(\mu\text{-}CO)(CO)_3$[b]	2.022 (1)	Mo Mo*	2.451 (1) 2.326 (1)	2.567 (1)	85.53 (3)	47.45 (3)	37
$Mn_2(\eta^2\text{-}\mu\text{-}MePS)(CO)_9$	2.033 (2)	Mn Mn*	2.289 (2) 2.394 (2)	2.414 (2)	129.4 (1)	51.1 (1)	38
$Os(\eta^2\text{-}PHS)(CO)_2(PPh_3)_2$	2.090 (5)		2.457 (3)[c] 2.443 (3)		50.5 (1)		

[a] 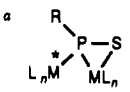

[b] R = *p*-$MeOC_6H_4$–. [c] See text.

Scheme II

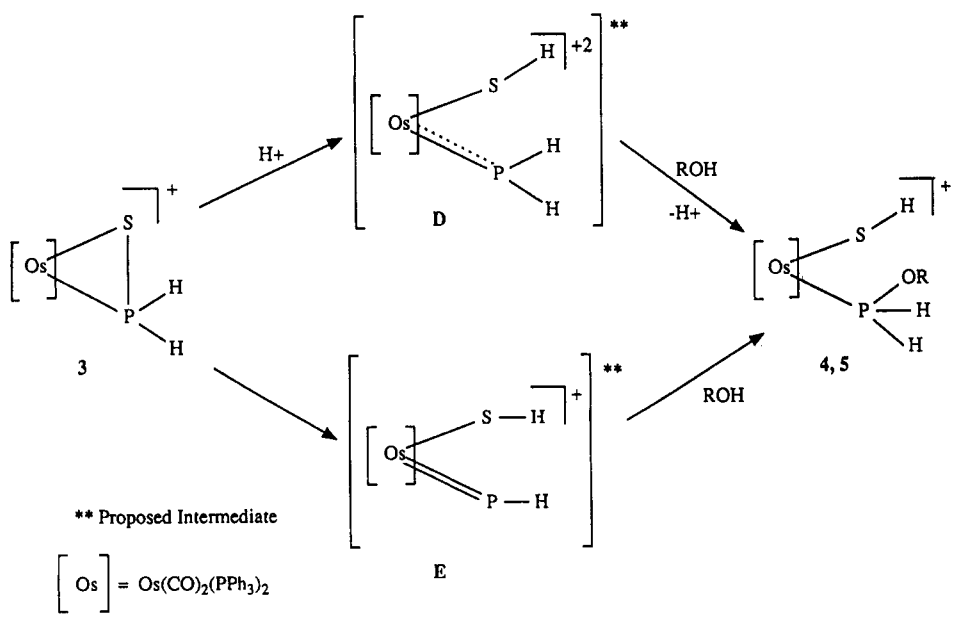

Scheme III

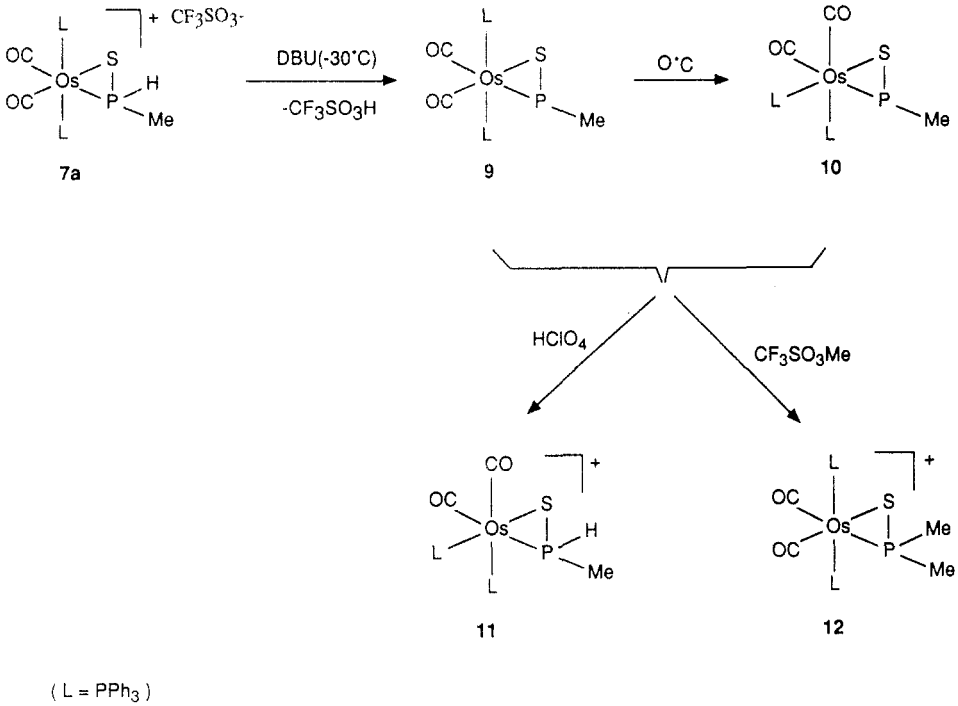

An alternative mechanism is that a terminal phosphinidene species (E) is generated, which then inserts into the O–H bond of an alcohol to give **4–6**. The latter is a well-established reaction for terminal phosphinidenes and their complexes.[14,15]

The phosphorus lone pairs in **2a,b** are readily alkylated by methyl triflate at room temperature to give the cationic complexes **7a,b** (eq 2). The air-stable complexes **7a,b**

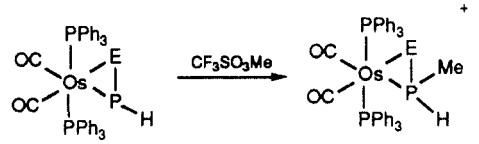

(2)

retain the P–E bonding, and the $^{31}P\{^1H\}$ NMR spectrum indicates that the geometry of the starting material remains intact during the reaction. Thus, the strong coupling of the mutually trans triphenylphosphine ligands present in **2a,b** is also found in **7a,b** with $^2J_{PP}$ = 229.2 and 227.2 Hz, respectively. Further chemistry of **7a** will be described below.

A second metal can be coordinated to the phosphorus in **2a**, and reaction of this complex with $[N(n\text{-}Bu)_4][AuI_2]$ gives the colorless adduct **8** (eq 3). Unfortunately the

$$\underset{\mathbf{2a}}{Os(\eta^2\text{-}PHS)(CO)_2(PPh_3)_2} \xrightarrow[-I^-]{[AuI_2]^-} \underset{\mathbf{8}}{Os(P(AuI)HS)(CO)_2(PPh_3)_2} \quad (3)$$

structure of **8** is not uniquely or unambiguously determined by spectroscopic means and we have not been able to obtain crystals suitable for X-ray diffraction. The ν(CO) bands in the IR spectrum are shifted to higher wavenumbers and indicate considerable reduction in the electron density at the metal. A phosphorus-bound proton is characterized by a stretching band at 2271 cm^{-1} in the IR spectrum and a signal at δ = 3.20 ppm (dt, 1, $^1J_{HP}$ = 343.9 Hz, $^3J_{HP}$ = 4.8 Hz) in the ^1H NMR spectrum. The ^{31}P NMR spectrum for **8** is temperature-dependent, and at room temperature it appears as two triplets that at −50 °C are transformed to a doublet for the triphenylphosphine ligands and a complex multiplet for the thioxophosphane resonance. These results suggest that either the product is not a simple gold iodide adduct as in F or, if it is, then

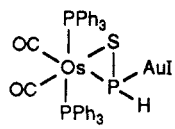

perhaps rapid $\eta^1 \leftrightarrow \eta^2$ interconversion is taking place. When ^1H and ^{31}P NMR spectra are used to monitor the in situ reaction represented by eq 3, **8** is shown to be rapidly produced as the only product. No other signals are observed. A structure in which AuI adopts a bridging position between P and S cannot be excluded.

Deprotonation of $[Os(\eta^2\text{-}PMeHS)(CO)_2(PPh_3)_2]^+$ (7a). As depicted in Scheme III, the η^2-methylphosphine sulfide complex **7a** reacts instantly with base to give the neutral methylthioxophosphane complex **9**. The complex **9** is surprisingly temperature-sensitive, and its solutions must be kept at temperatures less than −20 °C. Above this temperature products that result from the facile ligand sphere isomerization are produced. Thus, the characterization of **9** rests mainly upon the results of low-temperature NMR and IR spectroscopy of products isolated from the low-temperature preparation of **9**. Figure 5 depicts the variable-temperature results for solutions of **9** prepared at −30 °C in situ. The low-temperature spectrum corresponds to **9**, that is, it shows the methylthioxophosphane ligand cis to two mutually trans triphenylphosphine ligands. When the system is warmed to 0 °C, significant concentrations of a second isomer, **10**, are evident, which because of the reduced $^2J_{PP}$ coupling is formulated as containing a facial geometry of the three phosphorus donor ligands. Further warming to room temperature results in additional, but not complete, conversion of **9** and **10**.

(14) Marinetti, A.; Mathey, F. *J. Am. Chem. Soc.* **1983**, *104*, 4484.
(15) Bohle, D. S.; Roper, W. R. *J. Organomet. Chem.* **1984**, *273*, C4.

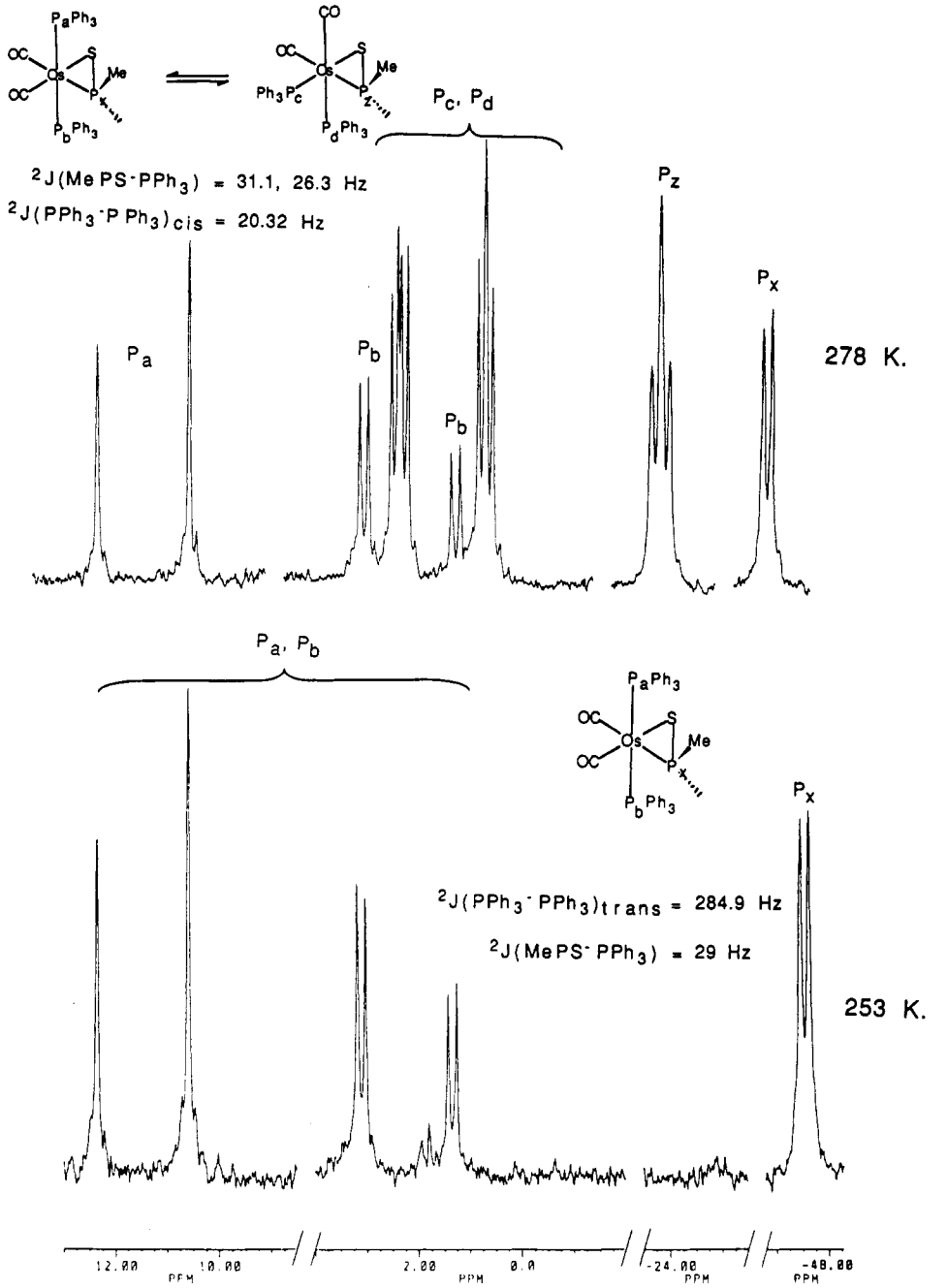

Figure 5. $^{31}P\{^1H\}$ NMR spectra for $Os(\eta^2\text{-}PMeS)(CO)_2(PPh_3)_2$ (**9**, **10**) at 253 and 278 K.

Recooling of this mixture to −73 °C freezes out the equilibrium concentrations of the isomers. Thus, **9** is a kinetic product that is in equilibrium with **10**, which is the more thermodynamically stable of the two products.

Reactions of solutions of **9** and **10** at equilibrium produce products whose geometries are electrophile-dependent. Reprotonation of the phosphorus in **9** ⇌ **10** specifically produces **11** with a facial geometry of the phosphorus donor ligands. This cationic complex is an isomer of **7a**, and it should be noted that **7a** was not found in the products of this reaction. On the other hand, methylation of the phosphorus lone pair in **9** ⇌ **10** gives a product that has equivalent triphenylphosphine ligands and cis carbonyl ligands. These features unambiguously define the geometry of **12** as one analogous to those of the structurally characterized **2a** and spectroscopically characterized **3a**.

The complexes **2a** and **9** ⇌ **10** as well as the series **3**, **7a**, **11**, and **12** allow for a comparison of effects of successive methylation upon the observed reactivity and structure in this class of complexes. In particular the contrast of **2a** and **9**, that is the thioxophosphane and methylthioxophosphane complexes, illustrates the enhanced lability of the coordination sphere with increasing methylation. This observation can be traced either to a steric effect, not only of the methyl group but also of the sterically active phosphorus lone pair, or to the availability of a low-energy $\eta^1 \leftrightarrow \eta^2$ MeP═S fluxionality. The cationic complexes with the formula $[L_nOs(\eta^2\text{-}RRP{=}S)]^+$, where R = H (**3**), R = H, R = Me (**7a**, **9**, **10**), and R = Me (**12**), also illustrate this effect, which is particularly pronounced in the synthesis of **12**. There is also an increasing stability toward hydrolysis or alcoholysis of the P–S bond with increasing methylation. Thus, while **3** is hydrolytically sensitive and reacts with alcohols, the remaining complexes can be recrystallized from alcohols and are stable in solution in the presence of excess acid. Thus, **7a**, **9**, and **10** did not form complexes analogous to **4**–**6** with alkyl methylphosphinite ligands, $[Os(SH)(PHMeOR)(CO)_2(PPh_3)_2]^+$.

Table IX. Gross Atomic Charges from a Mulliken Population Analysis of the RP=X Compounds[a]

molecule	P	R(-P)	X	H_1(-C)	H_2(-C)	H_1(-X)	H_2(-X)
HPO	+0.83	-0.12	-0.61				
HPS	+0.31	-0.06	-0.25				
HPSe	+0.49	+0.00	-0.49				
HPNH	+0.44	-0.07	-0.67			+0.30	
$HPCH_2$	+0.17	-0.07	-0.42			+0.16	+0.16
CH_3PO	+0.71	-0.44	-0.64	+0.14	+0.18		
CH_3PS	+0.26	-0.47	-0.27	+0.13	+0.17		
CH_3PSe	+0.62	-0.50	-0.37	+0.16	+0.17		
CH_3PNH	+0.49	-0.52	-0.74	+0.14	+0.14	+0.29	
CH_3PCH_2	+0.29	-0.49	-0.52	+0.14	+0.15	+0.15	+0.15

[a] See Figure 6 for the definitions of the atoms.

Ab Initio Calculations for RP=X. At the beginning of this work theoretical results for thioxophosphanes were limited to a study that focused on the energetics for isomerization of HP=S to PSH.[16] Considerably more information is available for oxophosphane,[17,18] and the frontier orbitals for the species HP=X (X = O, NH, CH_2) have been theoretically examined for their reactivity patterns with respect to [2 + 2] cycloaddition or condensation/cycloaddition by either [1 + 2] or [4 + 1] reaction.[19,20] The factors that determine the reactivity patterns are related to those which influence the character of these species as ligands. Thus, the ordering and constitution of the frontier orbitals not only control the reactivity patterns for these intermediates but also help to rationalize the binding modes for these species as ligands in the coordination sphere of transition metals. For a donor ligand the relative ordering of the occupied π and n(P) orbitals is particularly important and is reliably determined by ab initio SCF techniques. However, of equal importance for low-valent transition-metal complexes is the π-acceptor character of RP=X, and to assess this, the nature and relative energy of the LUMO orbitals are essential. In this section we present the results of our ab initio calculations for these species with the 6-311+G* basis set at both the Hartree–Fock (HF) level and the Møller–Plesset level, which includes electron correlation. Details of the calculations are included in the Experimental Section.

Figure 6 depicts the optimized ground-state equilibrium geometries for the species concerned. In each case a planar trans C_s symmetry was found for the hydrogens on P and X. Various trends that are found in these results are as follows. (1) There is an increase in the angle at the phosphorus in each case upon substitution of methyl for hydrogen. This trend is also experimentally found for the series of simple methylated phosphines from PH_3 to PMe_3.[21] Parallel results have also been found by Gordon et al. for substitution of H by Me, MeO, F, and NH_2 in HP=O.[22] Correction for electron correlation effects results in a consistent, but small, reduction of the R–P–X angle at the phosphorus. (2) Introduction of correlation in every case, except for HP=Se, lengthens the P=X bond and reduces the H–P bond length. (3) The H—P=X angle at phosphorus increases with increasing polarity of X.

In Table IX the gross atomic charges, calculated by a Mulliken population analysis at the HF level, indicate the pronounced positive charge localized on phosphorus in RP=X. Although this technique is at best qualitative, it

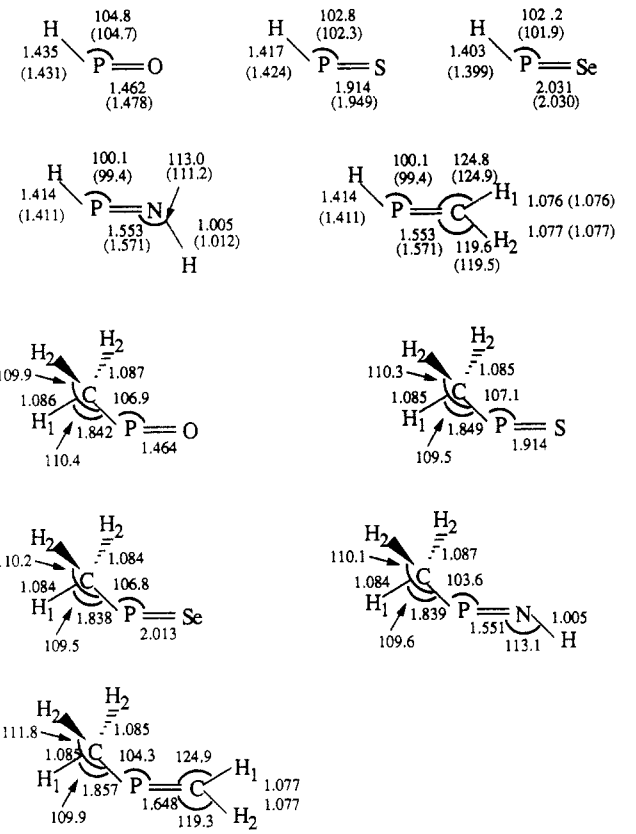

Figure 6. Ground-state structures for RP=X species (bond lengths in Å, angles in deg) as calculated with G-311+G* basis sets. Results at the MP2 level of electron correlation are given in parentheses.

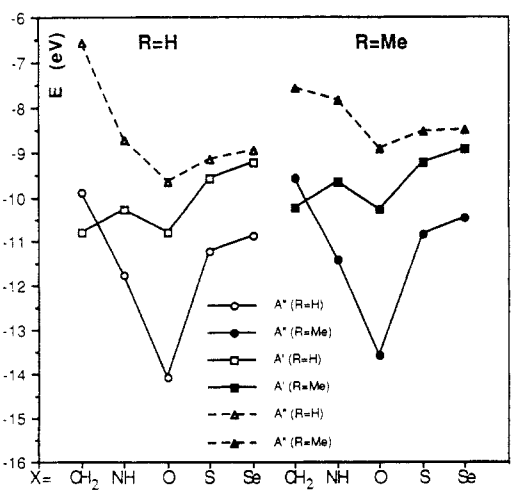

Figure 7. Frontier orbital energies (eV) for RP=X molecules.

(16) Boatz, J. A.; Gordon, M. S. *J. Comput. Chem.* **1986**, *7*, 306.
(17) Nguyen, M. T.; Hegarty, A. F.; Ha, T. K.; Brint, P. *Chem. Phys.* **1985**, *98*, 447.
(18) Gordon, M. S.; Binkley, J. S.; Pople, J. A.; Pietro, W. J.; Hehre, W. J. *J. Am. Chem. Soc.* **1982**, *104*, 2797.
(19) Schoeller, W. W.; Niecke, E. *J. Chem. Soc., Chem. Commun.* **1982**, 569.
(20) Schoeller, W. W.; Lerch, C. *Inorg. Chem.* **1986**, *25*, 576.
(21) Lappert, M. F.; Pedley, J. B.; Wilkins, B. T.; Stelzer, O.; Unger, E. *J. Chem. Soc., Dalton Trans.* **1975**, 1207.
(22) Gordon, M. S.; Boatz, J. A.; Schmidt, M. W. *J. Phys. Chem.* **1984**, *88*, 2998.

Table X. Total HF Energies (in au) for the Singlet (^{1}A′) and Triplet (^{3}A″) Ground States of the RP=X Compounds[a]

molecule	$E(^1A')$	$E(^3A'')$	T(ad)	T(v)
HPO	-416.132 393 (-416.324 552)	-416.108 205	63.5	109.7
HPS	-738.791 857 (-739.047 774)	-738.787 653	11.0	39.2
HPSe	-2 735.478 112 (-2 735.678 547)	-2 735.477 405	1.9	23.8
HPNH	-396.290 360 (-396.469 771)	-396.238 292	136.7	149.3
$HPCH_2$	-380.295 772 (-380.454 200)	-380.195 251	263.9	318.9
CH_3PO	-455.189 566	-455.156 152	87.7	130.5
CH_3PS	-777.843 295	-777.829 142	37.2	66.2
CH_3PSe	-2 774.529 108	-2 774.521 950	18.8	42.3
CH_3PNH	-435.343 082	-435.295 397	125.2	175.8
CH_3PCH_2	-419.339 927	-419.293 739	121.3	193.0

[a] The $E(^1A')$ MP2 values are given in parentheses. Adiabatic (ad) and vertical (v) $^1A' \rightarrow {}^3A''$ excitation energies T are in kJ/mol.

is informative in comparing closely related molecules. Methyl substitution results in greater negative charge localized on X, although the gross charge on the phosphorus in MeP=O and MeP=S is reduced, which may be explained by hyperconjugation of the methyl group with the polar P=X bond or by the +I effect of the methyl group.

The energies of the frontier orbitals are shown schematically in Figure 7. The orbital energies of the occupied orbitals can be related to the ionization energy via the Koopmans theorem. However, the unoccupied virtual orbitals are of only limited physical significance;[23] hence, we took the calculated singlet–triplet excitation energy to calculate the position of the first LUMO. The C_s symmetry of these species partitions the orbitals into a planar A′ set, for the σ and σ^* and n(P) nonbonding orbitals, and a A″ set, which contains the π and π^* orbitals for the P=X double bond. For the occupied orbitals there is a clear increase in the energies of both A′ and A″ levels for the methyl derivatives, the influence being particularly marked for the A′ orbitals of MeP=S. There is an inversion of the normal ordering of the HOMO and HOMO1 orbitals for $HP{=}CH_2$ so that the HOMO has A″ symmetry. This result is also found with small basis sets, although the use of reduced basis sets tends to underestimate the energies for the A′ level by as much as 1 eV for HP=NH.[19] Nevertheless, at all levels of theory there is an increase in the n(P) A′ energy with decreasing polarity of X in HP=X for the series X = O, NH, CH_2 as well as for X = O, S, Se.

The SCF energies for the LUMO's indicate that there is a very small difference, about 0.5 eV, between the lowest levels, which are ordered A″ < A′ except for $HPCH_2$, CH_3PO, and CH_3PCH_2. Since regular virtual HF orbitals do not describe very well the energy differences between the ground and excited states and the energies of such orbitals are very basis-set-dependent,[23] the triplet states arising from n(P) $\rightarrow \pi^*$(P=X) transitions were calculated for both fixed (singlet state) and relaxed geometries (Table X). The triplet ground state for all molecules has been determined to be of ^{3}A″ symmetry, as expected from the HOMO/LUMO order. The trends explained above remain qualitatively the same as obtained from the orbital energies, which supports the use of HOMO–LUMO difference pictures. Allowing for geometrical relaxation in the triplet state (adiabatic transition) lowers significantly the transition energy (Table XI). For example, the ^{3}A″ state of HPS shows an increase of 0.16 Å compared to the ^{1}A′ state. This can be related to the occupation of the π^* orbital. As a result, we expect also an increase in the P=X bond length if the bond to the osmium is due to a metal (π)–ligand (π^*) back-bond. Indeed, the X-ray analysis of **2a** results in a P=S bond distance of 2.09 Å, about 0.14 Å longer than the calculated MP2 value. The very low triplet excitation energy in HPSe is remarkable and indicates a very weak π(P=Se) bond. As a result, the change in the P=Se bond length is smallest in the HP=X (X = O, S, Se) series. The group state of this molecule could be the ^{3}A″ state; however, Nguyen showed for HPS that the ^{1}A′ $\rightarrow {}^3$A″ excitation energy increases by including electron correlation. CI calculations are necessary to get a more accurate description of this molecule.

In terms of rationalizing the observations of the HPS, HPSe, and MePS complexes **2a,b**, **9**, and **10** the relative energies in Figure 7 are very informative. The energy of the A′ n(P) level will largely determine the σ-donor character as a η^1-P-bound ligand (B). For metal fragments such as $Cr(CO)_5$ this η^1-σ-bound form is expected to be favored, and this is found in the complex $(OC)_5CrP(O)NR_2$.[5] Except for $HP{=}CH_2$ all the species are anticipated, on the basis of the relatively low-lying A′ levels, to be potential π donors when η^2-bound to a metal. The exceptions here are those that have phosphoryl bonds, P=O, where the strong π bonding results in very low-lying π orbitals and correspondingly high-lying LUMO's. The trend in the LUMO orbitals is significant and indicates that the progression HP=O < HP=S < HP=Se is expected for increasing π-acceptor ability. Comparing the MePX with HPX compounds, we see a decrease in the HOMO and an increase in the LUMO energy.

We are able to rationalize our observations of the relative stability of the complexes of HP=S and MeP=S toward isomerization by the results depicted in Figure 7. Methyl substitution results in a ligand that is a better σ donor but a poorer π acceptor than HP=S. Consequently, the transformation represented by B $\rightleftharpoons$ C is favored. The importance of π^* acceptance for HP=S is also illustrated by the geometry adopted for this ligand (Figure 4). More difficult to rationalize is the decrease in the P–H stretching band in the IR spectrum and the one-bond coupling in the NMR spectrum.

The results of our frequency analysis at the MP2 level are shown in Table XII. Nguyen[24] has used the experimental data for HPO to scale the calculated frequencies for HP=O and HP=S and predicted ν(H–P) in HP=S to be 2195 cm^{-1}. This is close to the observed value of 2196 cm^{-1} for the complex **2a**. The differences between the semiempirical scaled HF results of Nguyen and our MP2 values may give a measure of the accuracy of the MP2 frequency analysis.

Experimental Section

Standard Schlenk techniques were used in all preparations and reactions described. Otherwise, the new complexes described here can easily be handled in the open. General instrumental and experimental details have been described in previous publications.[25,26]

Preparation of New Compounds. Os(η^2-PHS)(CO)$_2$(PPh$_3$)$_2$ (2a). Os(η^1-OC(O)CH$_3$)(PH$_2$S)(CO)$_2$(PPh$_3$)$_2$[7] (**1a**; 0.5 g, 0.59 mmol) in 10 mL of dry THF was treated with CF_3SO_3H (1 equiv, 0.084 g, 0.049 mL). After addition there was no change in color or any outward sign of a reaction. DBU (3 equiv, 0.25 g, 0.25 mL, 1.7 mmol) was added immediately thereafter, and this instantly produced a bright yellow solution. This solution was stirred for 1 min, and then the THF was removed in vacuo. The residue

(23) Davidson, E. R.; Elbert, S. T.; Langhoff, S. R. *J. Chem. Phys.* **1972**, *57*, 1999, 2005.

(24) Nguyen, M. T. *Chem. Phys.* **1987**, *117*, 91.

(25) Bohle, D. S.; Roper, W. R. *Organometallics* **1986**, *5*, 1607.

(26) Bohle, D. S.; Clark, G. R.; Rickard, C. E. F.; Roper, W. R.; Taylor, M. J. *J. Organomet. Chem.* **1988**, *348*, 385.

Table XI. Triplet Vertical → Adiabatic Geometry Relaxation for RP=X[a]

	R = H					R = CH_3				
	X = O	X = S	X = Se	X = NH	X = CH_2	X = O	X = S	X = Se	X = NH	X = CH_2
Δr_{PX}	0.169	0.163	0.154	0.098	0.085	0.172	0.172	0.184	0.099	0.227
Δr_{PR}	−0.027	−0.009	−0.004	−0.007	−0.023	−0.009	0.022	0.012	0.026	0.006
Δr_{XH_1}				−0.005	−0.003				−0.010	−0.001
Δr_{XH_2}					−0.005					−0.001
Δr_{CH_1}						−0.003	−0.002	−0.002	−0.002	−0.001
Δr_{CH_2}						−0.003	−0.001	0.000	−0.003	0.000
$\Delta\alpha_{RPX}$	−11.3	−8.3	−6.8	−10.9	21.9	−10.8	−7.0	−7.3	−3.3	−4.2
$\Delta\alpha_{PXH_1}$				30.0	−2.4				31.3	3.5
$\Delta\alpha_{PXH_2}$					−3.5					−12.9
$\Delta\alpha_{CH_1}$						1.8	3.4	−1.1	−1.2	2.3
$\Delta\alpha_{CH_2}$						−0.7	−1.1	0.9	−0.1	−1.7

[a] Changes in X–Y bond distances $\Delta r_{XY} = r_{XY}(^3A'') - r_{XY}(^1A')$ are in Å; changes in X–Y–Z bond angles $\Delta\alpha_{XYZ} = \alpha_{XYZ}(^3A'') - \alpha_{XYZ}(^1A')$ are in degrees.

Table XII. Vibrational Frequencies ν_e in cm^{-1} from MP2 Harmonic Force Fields for the HP=X Compounds (X = O, S, Se, NH, CH_2)

	mode			
molecule	H–P	P–X	H–P–X	others
HPO	2410	1286	869	
HPO (exptl)	2345	1188	985	
HPS	2345	721	624	
HPS (ref 24)	2193	879	667	
HPSe	2570	728	589	
HPNH	2536	1337	775	NH 3583, PNH 1094
$HPCH_2$	2412	1212	792	CH_1 3273, CH_2 3168, PCH_1 1116, PCH_2 921

was taken up in 40 mL of dichloromethane, and 40 mL of ethanol was added. Concentration of this mixture resulted in the formation of fine light yellow prisms. Filtration, and a thorough wash with methanol, ethanol, and finally *n*-hexane, afforded 0.31 g (63%) of the product, mp 188–189 °C. Anal. Found: C, 53.25; H, 4.32. Calcd for $C_{38}H_{31}O_2OsP_3S$: C, 53.33; H, 3.70. Hexagonal crystals suitable for X-ray diffraction were grown from dichloromethane/ethanol under nitrogen.

Os(η^2-PHSe)(CO)$_2$(PPh$_3$)$_2$ (2b). Os(η^1-OC(O)CH_3)(PH_2Se)$(CO)_2(PPh_3)_2$[7] (**1b**; 0.35 g, 0.37 mmol) was sequentially treated with 1 equiv of CF_3SO_3H (0.37 mmol, 0.056 g, 0.033 mL) and DBU (3 equiv, 1.11 mmol, 0.169 g, 0.160 mL) as described above for **2a**. This afforded yellow-orange plates of **2b** (0.23 g, 0.26 mmol, 70%) after recrystallization from dichloromethane/ethanol; mp 167 °C. Anal. Found: C, 51.13; H, 4.14. Calcd for $C_{38}H_{31}O_2OsP_3Se$: C, 51.76; H, 3.55.

[Os(SH)(PH$_2$OMe)(CO)$_2$(PPh$_3$)$_2$]ClO$_4$ ((4)ClO$_4$). Os(η^2-PHS)$(CO)_2(PPh_3)_2$ (**2a**; 0.08 g) in 10 mL of dichloromethane was treated with a 5-mL solution prepared from 0.2 mL of aqueous perchloric acid and 5 mL of methanol. Addition of the acid caused the instant dissolution of the pale yellow starting material and formation of a colorless solution. This mixture was stirred for 30 min, and then 20 mL each of ethanol and 2-propanol were added and the solution was concentrated to less than a 10-mL volume. The resulting plates were filtered and washed with 2-propanol and *n*-hexane to give 0.09 g (100%) of **4**. This compound was spectroscopically characterized (Tables VI and VII).

[Os(SH)(PH$_2$OEt)(CO)$_2$(PPh$_3$)$_2$]ClO$_4$ ((5)ClO$_4$). Os(η^2-PHS)$(CO)_2(PPh_3)_2$ (**2a**; 0.06 g) was suspended in 10 mL of dichloromethane and was treated with a solution of 0.2 mL of aqueous perchloric acid in 10 mL of ethanol. The pale yellow suspension dissolved instantly to give a colorless solution. After this solution was stirred for 1 h, 15 mL of 2-propanol was added and crystallization was induced by concentration of this mixture in vacuo. Filtration afforded 0.07 g (96%) of large plates, mp 169–170 °C. Anal. Found: C, 48.07; H, 4.92. Calcd for $C_{40}H_{38}ClO_7OsP_3S$: C, 48.21; H, 3.88.

[Os(SeH)(PH$_2$OEt)(CO)$_2$(PPh$_3$)$_2$]ClO$_4$ ((6)ClO$_4$). Os(η^2-PHSe)$(CO)_2(PPh_3)_2$ (**2b**; 0.5 g) was suspended in 2 mL of dichloromethane, and a 10-mL solution of 0.2 mL of aqueous perchloric acid in ethanol was added. The orange-yellow suspension faded rapidly to give a slightly yellow solution, from which a tan colored product could be isolated as described for **5**. The yield from this reaction was low (<40%), and this product can only be recrystallized in the presence of acid; mp 144 °C. Anal. Found: C, 45.73; H, 4.10. Calcd for $C_{40}H_{38}ClO_7OsP_3Se$: C, 46.72; H, 3.73.

[Os(η^2-PHMeS)(CO)$_2$(PPh$_3$)$_2$]CF$_3$SO$_3$ ((7a)CF$_3$SO$_3$). Os(η^2-PHS)$(CO)_2(PPh_3)_2$ (**2a**; 0.07 g, 0.084 mmol) was suspended in 10 mL of *dry* dichloromethane, and 2 equiv of methyl triflate (0.17 mmol, 0.027 g, 0.019 mL) was added. This mixture was stirred at room temperature for 10 min, during which time the pale yellow solid dissolved and a colorless solution formed. After an additional 30 min at room temperature all of the volatile components of the reaction mixture were removed and the system was held under vacuum for a further 2 h. The dry colorless residue was taken up in 10 mL of dichloromethane and then recrystallized by addition of 10 mL of ethanol and concentration of this mixture. Large colorless crystals of the product (0.08 g, 95%) were recovered by filtration and were washed with ethanol and *n*-hexane; mp 167 °C. Anal. Found: C, 47.26; H, 4.03. Calcd for $C_{40}H_{34}F_3O_5OsP_3S_2$: C, 47.38; H, 3.42.

[Os(η^2-PHMeSe)(CO)$_2$(PPh$_3$)$_2$]CF$_3$SO$_3$ ((7b)CF$_3$SO$_3$). Os(η^2-PHSe)$(CO)_2(PPh_3)_2$ (**2b**; 0.11 g, 0.12 mmol) was treated with 1.5 equiv of methyl triflate (0.19 mmol, 0.031 g, 0.022 mL), as described for the preparation of **7a**. The resulting tan residue was taken up in dichloromethane, and the product was recovered by addition of 10 mL of *n*-hexane and recrystallization of this mixture in vacuo. The product had a slight yellow color, and it was necessary to recrystallize this material in the presence of perchloric acid. As a consequence, its characterization was based mainly on the similarity of the spectral data for this product with those of **7a**.

Os(PH(AuI)S)(CO)$_2$(PPh$_3$)$_2$ (8). Os(η^2-PHS)$(CO)_2(PPh_3)_2$ (**2a**; 0.042 g, 0.050 mmol) and 1 equiv of $[N(n\text{-}Bu)_4][AuI_2]$[27] (0.05 mmol, 0.035 g) were stirred together in 10 mL of dichloromethane, whereupon both solids dissolved instantly to give a colorless solution. This solution was stirred for 1 h at room temperature, and the product was crystallized by the addition of 10 mL of ethanol followed by concentration in vacuo. Colorless needles (0.07 g, 96%) were obtained by filtration and a thorough washing with ethanol and *n*-hexane; mp 190 °C. Anal. Found: C, 40.81; H, 3.59. Calcd for $C_{38}H_{31}AuIO_2OsP_3S$: C, 40.50; H, 3.78.

***trans*-Os(η^2-PMeS)(CO)$_2$(PPh$_3$)$_2$ (9).** Under a nitrogen atmosphere $[Os(\eta^2\text{-}PHMeS)(CO)_2(PPh_3)_2]CF_3SO_3$ ((**7a**)CF_3SO_3; 0.13 g) was dissolved in 6 mL of dichloromethane and 5 mL of

(27) Braunstein, P.; Clark, R. J. H. *J. Chem. Soc., Dalton Trans.* **1973**, 1845.

ethanol was added. DBU (excess, 0.1 mL) was added, and the solution instantly became bright yellow. Immediately the solvent volume was reduced and fine yellow crystals rapidly formed. This material was recovered by filtration and successive washes with ethanol and *n*-hexane. It was not possible to recrystallize this material at room temperature under nitrogen, or in the open, as instead the isomer **10** was recovered.

***cis*-Os(η^2-PMeS)(CO)$_2$(PPh$_3$)$_2$ (10).** [Os(η^2-PHMeS)(CO)$_2$(PPh$_3$)$_2$]CF$_3$SO$_3$ (**(7a)**CF$_3$SO$_3$; 0.12 g) was suspended in 10 mL of dry, oxygen-free benzene. Excess DBU (0.1 mL) was added, and the white suspension gradually dissolved to give a pale yellow solution. Ethanol (20 mL) was added, and after concentration very fine pale crystals of **10** formed. After filtration, the product (0.08 g, 72%) was washed thoroughly with ethanol and then *n*-hexane. As with **9**, the basis for the characterization of this product was derived from in situ NMR experiments.

***cis*-[Os(η^2-PHMeS)(CO)$_2$(PPh$_3$)$_2$]ClO$_4$ ((11)ClO$_4$).** Os(η^2-PMeS)(CO)$_2$(PPh$_3$)$_2$ (0.05 g), as a mixture of **9** and **10** at room temperature in dichloromethane, was treated with 0.1 mL of aqueous perchloric acid in 10 mL of methanol. There was an instant loss of the bright yellow color, and after 1 h the product (0.05 g, 89%) was crystallized as large colorless cubes after addition of 10 mL each of ethanol and 2-propanol and concentration in vacuo; mp 175 °C. Anal. Found: C, 49.35; H, 4.30. Calcd for C$_{39}$H$_{34}$ClO$_6$OsP$_3$S: C, 49.34; H, 3.62.

[Os(η^2-PMe$_2$S)(CO)$_2$(PPh$_3$)$_2$]CF$_3$SO$_3$ ((12)CF$_3$SO$_3$). Os(η^2-PMeS)(CO)$_2$(PPh$_3$)$_2$ (0.12 g) as a mixture of **9** and **10** in a 2-mL dichloromethane solution was treated with 2 equiv of methyl triflate (0.046 g, 0.032 mL, 0.28 mmol). There was an instantaneous loss of the bright yellow color, and after 1 min the solvent was removed and the residue was kept under a high vacuum for 1 h. The residue was taken up in 2 mL of dichloromethane, and 50 mL of *n*-hexane was then added to precipitate the product from solution (0.07 g, 84%). Large colorless crystals were grown from dichloromethane/ethanol, and the sample for microanalysis was obtained from this solvent pair; mp 160–162 °C. Anal. Found: C, 48.84; H, 4.16. Calcd for C$_{41}$H$_{36}$F$_3$O$_5$OsP$_3$S$_2$: C, 48.61; H, 3.59.

Reaction of Os(η^2-PHS)(CO)$_2$(PPh$_3$)$_2$ with CF$_3$SO$_3$H and the Formation of [Os(η^2-PH$_2$S)(CO)$_2$(PPh$_3$)$_2$]CF$_3$SO$_3$ ((3a)CF$_3$SO$_3$). Os(η^2-PHS)(CO)$_2$(PPh$_3$)$_2$ (**2a**) was dissolved in dry deuteriochloroform under nitrogen in a NMR tube. One equivalent of trifluoromethanesulfonic acid, as a solution in deuteriochloroform, was then added, and the spectrum was acquired immediately. For the ^{31}P{^{1}H} NMR experiment DBU was then added after 5 min and the spectrum reacquired. This latter experiment demonstrated that the resonances attributed to **3a** disappear and the resonances due to **2a** reappear. The ^{31}P{^{1}H} NMR spectrum of **3a** was also obtained by treating **1a** with trifluoromethanesulfonic acid. After 5 min this sample was treated with DBU to give a light yellow solution, which had resonances attributable to **2a**.

Variable-Temperature ^{31}P{^{1}H} NMR Experiments for Os(η^2-PMeS)(CO)$_2$(PPh$_3$)$_2$ (9, 10). [Os(η^2-PHMeS)(CO)$_2$(PPh$_3$)$_2$]CF$_3$SO$_3$ (**(7a)**CF$_3$SO$_3$) was suspended in dry degassed C$_6$D$_5$CD$_3$ in a NMR tube, and the tube was immersed in a dry ice/acetone bath and cooled to 195 K. Immediately before this sample was placed into the previously cooled NMR probe, excess DBU was added, and a light yellow solution formed within several seconds. The temperatures of the sample and the probe were then gradually raised to room temperature with spectral data acquisition at every 15 K. There was no change in the spectra acquired in this manner until the temperature was raised to 295 K.

X-ray Diffraction Study of 2a. The unit cell was determined from a least-squares fit of four-circle angles in the range $20° < 2\theta < 24°$. Crystal data and refinement details are given in Table XIII. Space group $P\bar{1}$ was assumed and confirmed by the successful structure solution and refinement. The position of the osmium atom was determined by Patterson methods, the remaining atoms were found from successive difference Fourier maps, and the model was refined by full-matrix least squares with use of SHELX-76. Attempts to distinguish between the phosphorus and sulfur atoms of the HPS group were unsuccessful. Refinement with atoms assigned individually as phosphorus and sulfur (or vice versa) produced no significant differences in residual and thermal parameters. Accordingly, these atoms were treated as an average of the two. Anisotropic thermal parameters were refined for all atoms except the phenyl carbon atoms, but hydrogen atoms were omitted. Bond distances, bond angles, and final positional parameters are given in Tables III–V, respectively. Further details are available on request from Cambridge Crystallographic Data Centre, University Chemical Laboratory, Lensfield Road, Cambridge CB2 1EW, U.K.

Table XIII. Crystal Data for Os(η^2-HPS)(CO)$_2$(PPh$_3$)$_2$

formula	C$_{38}$H$_{31}$O$_2$OsP$_3$S
fw	835.44
temp	291 ± 1 K
space group	$P\bar{1}$
a	10.524 (4) Å
b	18.010 (3) Å
c	10.389 (5) Å
α	103.26 (3)°
β	115.63 (3)°
γ	76.11 (2)°
V	1705.6 (2) Å^3
D	1.62 g cm^{-3} (Z = 2)
yellow hexagonal prisms	0.25 × 0.20 × 0.15 mm
diffractometer	Nonius CAD-4
radiation	Zr-filtered Mo Kα (λ = 0.71069 Å)
scan type	2θ–θ
2θ scan limits	$2° < \theta < 46°$
scan limits	$-11 < h < 11$, $-19 < k < 19$, $-11 < l < 0$
std rflns	3 measd every 100 rflns, no indication of cryst decay
total no. of rflns surveyed	5066
no. of unique rflns ($I > 3\sigma(I)$)	3455
merging residual	0.021
abs cor	empirical ϕ scans
linear abs coeff	41.8 cm^{-1}
transmissn factor range	0.894–0.999
scattering factors	ref 39
R	0.039
R_w	0.041
weights	$1.24/(\sigma^2(F) + 0.001F^2)$

Theoretical Methods. The method used is similar to that described previously by Nguyen for the molecule HPS.[24] The HF calculations for the ^{1}A′ ground state and ^{3}A″ excited state and the MP2 calculations for the ^{1}A′ ground state of the RP=X compounds have been performed with use of the program package GAUSSIAN86.[28] The full active MP2 space has been used. Unrestricted HF has been employed for the triplet states. The geometry optimization has been performed with use of gradient procedures. The basis sets used are 31+G* for H, 631+G* for C, N, and O, 6631+G* for P and S, and (62211s, 42111p, 3111d) for Se. For example, for the ^{3}A″ state of CH$_3$PSe 197 primitive Gaussians contracted to 98 basis functions have been used; a Berny geometry optimization[28] (seven points on the hypersurface) took about 10 h on an IBM 3081 computer. The vibrational analysis has been performed with use of Wilson's symmetry-adapted GF-matrix method.[29,30]

(28) Frish, M. J.; Binkley, J. S.; Schlegel, H. B.; Raghavachari, K.; Melius, C. F.; Martin, L.; Stewart, J. J. P.; Bobrowicz, F. W.; Rohlfing, C. M.; Kahn, L. R.; DeFrees, D. J.; Seeger, R.; Whiteside, R. A.; Fox, D. J.; Fluder, E. M.; Pople, J. A. Program GAUSSIAN86; Carnegie-Mellon Quantum Chemistry Publishing Unit: Pittsburgh, PA, 1984.

(29) Wilson, E. B.; Decius, J. C.; Cross, P. C. *Molecular Vibrations, The Theory of Infrared and Raman Vibrational Spectra*; McGraw-Hill: London, 1955.

(30) Schwerdtfeger, P.; Bowmaker, G. A.; Boyd, P. D. W.; Earp, C. D.; Hannon, S. F. Program VIB; Department of Chemistry, University of Auckland: Auckland, New Zealand, 1987.

(31) Collins, T. J.; Grundy, K. R.; Roper, W. R. *J. Organomet. Chem.* **1982**, *231*, 161.

(32) Grundy, K. R.; Roper, W. R. *J. Organomet. Chem.* **1976**, *113*, C45.

(33) Clark, G. R.; Russell, D. R.; Roper, W. R.; Walker, A. *J. Organomet. Chem.* **1977**, *136*, C1.

(34) Farrar, D. H.; Grundy, K. R.; Payne, N. C.; Roper, W. R.; Walker, A. *J. Am. Chem. Soc.* **1979**, *101*, 6577.

(35) Grundy, K. R.; Roper, W. R. *J. Organomet. Chem.* **1981**, *216*, 255.

(36) Hussong, R.; Heydt, H.; Maas, G.; Regitz, M. *Chem. Ber.* **1987**, *120*, 1263.

(37) Alper, H.; Einstein, F. W. B.; Petrignani, J. F.; Willis, A. C. *Organometallics* **1983**, *2*, 1422.

Acknowledgment. P.S. thanks the Alexander von Humboldt Stiftung (Bonn, West Germany) for financial support. D.S.B. thanks the New Zealand Universities Grants Committee for the award of a Postgraduate Scholarship, and we are indebted to the Center for Information Science (University of Auckland) and to IBM New Zealand Ltd. for providing large amounts of computer time.

(38) Lindner, E.; Auch, K.; Hiller, W.; Fawzi, R. *Angew. Chem., Int. Ed. Engl.* **1984**, *23*, 320.
(39) *International Tables for X-Ray Crystallography*; Kynoch Press: Birmingham, England, 1974; Vol. IV.

Supplementary Material Available: Tables of thermal parameters and all bond lengths and angles for **2a** (5 pages); a table of observed and calculated structure factors (15 pages). Ordering information is given on any current masthead page.

Pentacoordinated Silicon Anions: Synthesis and Reactivity[1]

Jean-Louis Bréfort, Robert J. P. Corriu,* Christian Guérin, Bernard J. L. Henner, and Wong Wee Choy Wong Chi Man

Laboratoire "Hétérochimie et Amino-Acides", UA CNRS 1097, Université de Montpellier II, Sciences et Techniques du Languedoc, Place Eugène Bataillon, F-34095 Montpellier Cedex 5, France

Received January 4, 1990

Pentacoordinated anionic siliconates $Ph_3Si(OMe)_2^-K^+$(18-crown-6), $Ph_2Si(OMe)_3^-K^+$(18-crown-6), $Ph_3SiF_2^-K^+$(18-crown-6), and $MePhSiF_3^-K^+$(18-crown-6) reacted with nucleophiles (RMgX, RLi, ROLi, $LiAlH_4$) to give the neutral tetravalent substituted silicon derivatives. Reactivity comparisons between $Ph_3SiX_2^-K^+$(18-crown-6) and Ph_3SiX (X = F, OMe) showed that the pentavalent anionic species is more reactive than the tetravalent analogue toward nucleophiles. Hydrolysis reactions of $Ph_3SiF_2^-K^+$(18-crown-6) and $Ph_3Si(OMe)_2^-K^+$(18-crown-6) gave respectively Ph_3SiF and a mixture of Ph_3SiOMe and Ph_3SiOH. Results clearly indicate that nucleophilic attack at pentacoordinated silicon species is a general process. Moreover, the data point out the enhanced reactivity of these species that may mainly arise from a general loosening of the bonds around silicon.

Over the last 20 years interest in hypervalent silicon compounds has grown considerably, and many isolable organosilicon compounds with coordination number greater than 4 are known.[2]

Our interest in the reactivity of pentacoordinated anionic silicon species is derived from several sources.

(1) Nucleophilic displacements in tetravalent organosilicon derivatives, R_3SiX, have been assumed to pass through the formation of a pentacoordinated anionic silicon intermediate.[3]

(2) Nucleophilic displacement at silicon can be activated by catalytic amounts of nucleophiles that are good coordinating agents for silicon.[3,4] The rate-determining step of the proposed mechanism (Scheme I) is attack of the nucleophile Nu^- at a pentacoordinated silicon center.

(3) The reaction of silicon hydrides, $RSiH_3$ and R_2SiH_2, with KH as a catalyst gives redistribution processes that are interpreted as involving intermediate formation of a pentacoordinated silicon complex.[5] In the same way, fast racemization of MePh-1-NpSiH(D), (1-Np = 1-naphthyl) catalyzed by hydrides (KH, $LiAlH_4$, $LiAlD_4$) was rationalized through formation of a pentacoordinated hydridoorganosiliconate anion.[6]

Scheme I

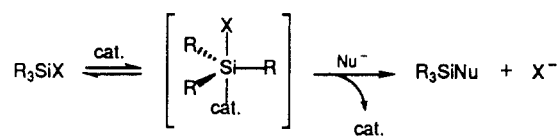

cat. = F, $RCOO^-$, HMPA

(4) The reduction of carbonyl compounds with silicon hydrides and fluoride[7] or alcoholate[8] ions as activators is well-known and proceeds through a pentacoordinated silicon intermediate. Recently anionic hydridosilicates have been isolated and have been shown to be the active species in the reduction of carbonyl compounds.[9,10] Finally, the intramolecularly coordinated silicon dihydride **1** has also been shown to possess a much more reactive hydrogen function than 1-naphthylphenylsilane.[11,12]

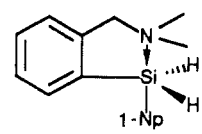

1

(1) Preliminary communication: Corriu, R. J. P.; Guérin, C.; Henner, B. J. L.; Wong Chi Man, W. W. C. *Organometallics* **1988**, *7*, 237.
(2) For a review see: Hypervalent Silicon Compounds. In *The Chemistry of Organic Silicon Compounds*; Patai, S., Rappoport, Z., Eds.; Wiley: New York, 1989; Chapter 20, p 1242.
(3) Corriu, R. J. P.; Guérin, C. *J. Organomet. Chem.* **1980**, *198*, 232; *Adv. Organomet. Chem.* **1982**, *20*, 265. Corriu, R. J. P.; Guérin, C.; Moreau, J. *Top. Stereochem.* **1982**, *15*, 43; Dynamic Stereochemistry at Silicon. In *The Chemistry of Organic Silicon Compounds*; Patai, S., Rappoport, Z., Eds.; Wiley: New York, 1989; Chapter 4, pp 306-370.
(4) Corriu, R. J. P.; Dabosi, G.; Martineau, M. *J. Chem. Soc., Chem. Commun.* **1977**, 649; *J. Organomet. Chem.* **1978**, *150*, 27; **1978**, *154*, 33.
(5) Becker, B.; Corriu, R. J. P.; Guérin, C.; Henner, B. J. L. *J. Organomet. Chem.* **1989**, *369*, 147.
(6) Bréfort, J. L.; Corriu, R. J. P.; Guérin, C.; Henner, B. J. L. *J. Organomet. Chem.* **1989**, *370*, 9.
(7) Boyer, J.; Corriu, R. J. P.; Perz, R.; Reye, C. *Tetrahedron* **1981**, *37*, 2165. Boyer, J.; Corriu, R. P. J.; Perz, R.; Poirier, M.; Reye, C. *Synthesis* **1981**, 558. Chuit, C.; Corriu, R. J. P.; Perz, R.; Reye, C. *Ibid.* **1982**, 981. Corriu, R. J. P.; Perz, R.; Reye, C. *Tetrahedron* **1983**, *39*, 999. Fujita, M.; Hiyama, T. *J. Am. Chem. Soc.* **1984**, *106*, 4629; **1985**, *107*, 8294; *Tetrahedron Lett.* **1987**, *28*, 2263.
(8) Kohra, S.; Hayashida, Y.; Tominaga, Y.; Hosomi, A. *J. Chem. Soc., Chem. Commun.* **1986**, 1411; *Tetrahedron Lett.* **1988**, *29*, 89.
(9) Kira, M.; Sato, K.; Sakurai, H. *Chem. Lett.* **1987**, 2243; *J. Org. Chem.* **1987**, *52*, 948.
(10) Becker, B.; Corriu, R. J. P.; Guérin, C.; Henner, B. J. L.; Wang, Q. *J. Organomet. Chem.* **1989**, *368*, C25.
(11) Boyer, J.; Brelière, C.; Corriu, R. J. P.; Kpoton, A.; Poirier, M.; Royo, G. *J. Organomet. Chem.* **1986**, *311*, C39.

0276-7333/90/2309-2080$02.50/0